

Robust control and state observer design for neural mass model applications using simulated EEG signals

Andrei Popescu * Catalin Buiu *

* *Automatic Control System Engineering Department, Faculty of Automatic and Computer Science of National University of Science and Technology Politehnica Bucharest, 313 Splaiul Independentei, Bucuresti 060042, Romania, (emails: andrei.popescu0102@upb.ro and catalin.buiu@upb.ro)*

Abstract: The paper presents, on the one hand, the design of a robust control method using H_∞ tools applied to a nonlinear neural mass model of a cortical column using EEG recordings as signal measurements. The objective of the control problem is to suppress the neuronal activity of the cortical column by ensuring guaranteed performance specifications as well as robustness against model uncertainties and measurement noise. On the other hand, to monitor the hidden, unmeasured, activity of a cortical column an Extended Kalman Filter is designed based on the neural mass model of the macrocolumn and EEG measurements of its activity. The capabilities of these methods are tested, in simulation, using the neural mass model description of a cortical column for an epileptic seizure. Both methods, the robust controller and the state observer, show promising results in simulation.

Keywords: neural mass model; convolution-based model; robust control problem; H_∞ tools; estimation problem; extended Kalman filter; nonlinear observer application; EEG recordings; epileptic seizure model;

1. INTRODUCTION

Neural mass models have been extensively used to study and understand the dynamics of the neuronal populations of the cerebral cortex, also known as the gray matter of the brain. Even though often the neural mass models, for some parameters ranges, fail to fully grasp the dynamics of the neural networks as detailed in Deschle et al. (2021), their study can still be fruitful to advance the understanding of the brain.

In particular, they can be useful to be considered as proxy for the real neural networks dynamics, in simulation, if one is interested to apply, test and analyze different techniques often used in control system engineering such as state observers or controller design. The insights gain conducting such studies can broaden the horizon of biomedical engineering and research, especially nowadays when the medical and engineering fields work together to study or solve problems that were impossible to be tackled in the past.

Traditionally, the neural mass models are built by using one of the two methods: the convolution-based model Jansen and Rit (1995) or conductance-based one Hodgkin

and Huxley (1952). Both of them have the same goal, that is to describe the mean activity of an otherwise large neuronal population, by using a reduced number of state variables. Applications based on these approaches have been developed to demonstrate the capabilities of these models. The former had been exploited in David and Friston (2003) and David et al. (2006) to mimic narrow-band brain oscillations and event-related activity, while in Moran et al. (2007) and Moran et al. (2013) to reproduce the steady-state responses of the brain. The latter had been described in Pereira et al. (2021) how it can be used in the context of dynamic causal modelling for cross-power spectral densities.

Furthermore, the electrical brain activity can be measured by using electroencephalogram (EEG) sensors. More detailed, these electrodes placed on the scalp measure the postsynaptic potential (PSP) of the pyramidal neurons as it can be find in Glomb et al. (2022). Therefore, one can built neural mass model so as to replicate the measured electrical activity of a so-called cortical column.

The aim of this paper is twofold: firstly, an H_∞ controller is designed to suppress the activity of a cortical column, in particular applied to an epileptic seizure neural mass model of the macrocolumn. The solution is computed based on the linearization model of the nonlinear neural mass model and it takes into account the model uncertainties as additive ones, as well as the measurement noise. Secondly, to design a state observer for the same application, in order to monitor the hidden, unmeasured

* The results presented in this paper, on the one hand, have been funded by the Ministry of Investments and European Projects through the Human Capital Sectoral Operational Program 2014-2020, Contract no. 62461/03.06.2022, SMIS code 153735, and on the other hand, supported by a grant of the Ministry of Research, Innovation and Digitization, CNCS-UEFISCDI, project number PN-III-P1-1.1-PD-2021-0285, within PNCDI III.

state of the cortical column. To that end, an Extended Kalman filter is put in place. Both of them represent also the main contributions of the paper, since to the best of our knowledge, there are no such solutions presented for the neural mass model of the epileptic seizure. The proposed methods are testes in simulation.

It is worth noticing that other attempts to suppress the activity of a cortical column in an epileptic seizure have been made by using, in one instance, a PI controller Wang et al. (2016) and in another, an active disturbance rejection control Wei et al. (2019). Both of them were tested in simulation with promising results. As for the estimation problem, one can find as well attempts to solve it, in particular Hamid et al. (2015), Kuhlmann et al. (2016) and Popescu and Buiu (2023), but none of them is applied for the neural mass model of an epileptic seizure, or the extended Kalman filter, for that matter.

The paper is organized as follows. In Section 2, the detailed mathematical model of the cortical column of an epileptic seizure is given, in terms of a convolution-based neural mass model, which was introduced in Wendling et al. (2000). In Section 3, the H_∞ controller solution is presented, particularized for the neural mass model in discussion, while in Section 4, the extended Kalman filter is described as a solution for the estimation problem formulated in this paper. Furthermore, in Section 5, the simulation results for both, the control and estimation problems are shown. Finally, Section 6, concludes the paper.

2. NEURAL MASS MODEL OF A CORTICAL COLUMN

The goal of this section is to describe a cortical column as a neural mass model. The main idea is to approximate a large number of neurons as a representative population and to use the behaviour of that neuronal population to compute the average activity of the correspondent group. The advantage of this representation is that it needs a reduced number of state variables to approximate a fairly sizeable number of neurons. The mathematical model of a cortical column will be given in the general form of a dynamical system as expressed by the following equations:

$$\begin{aligned} \dot{x}(t) &= f(x(t), u(t), \theta) + w(t) \\ y(t) &= h(x(t)) + n(t) \end{aligned} \quad (1)$$

where $x(t) \in \mathbb{R}^n$ represents the hidden state of the dynamical system (the neuronal populations activity), $\dot{x}(t) \in \mathbb{R}^n$ is the first time derivative of the state vector, $u(t) \in \mathbb{R}^m$ is the external deterministic input to the neural populations (i.e. particular stimuli presented to the cortical column which can be in form of an evoked potential of a specific experimental manipulators or an electrical current/magnetic impulse applied using a specialized technique). Their roll is to generate the brain's response to specific external manipulators. Next, θ gathers the information about the model parameters. On top of that, the function $f(\bullet) \in \mathbb{R}^n$ maps the relations between all these variables.

Furthermore, $y(t) \in \mathbb{R}^p$ represents the measured output, which in this case is the EEG recordings. Additionally, the function $h(\bullet) \in \mathbb{R}^p$ describes how the neural populations

activity propagates through the surroundings tissues such as skull, scalp, or the brain itself.

Finally, the dynamical system description includes the signals $w(t)$ and $n(t)$ which represent the disturbances of the state, respectively, the measurement noise. These variables can be stochastic. The first equation of (1) is called the neuronal model, while the second one is the observational model.

One way to obtain the neural mass model of a cortical column is using the convolution-based description of a three populations Jansen-Rit model which has been introduced in Jansen and Rit (1995) and will be briefly presented as part of the following section.

2.1 Jansen-Rit model

In its original form, the cortical column local circuit (one source) has been described as a interaction of three populations of neurons. More precise, the main population comprised of the pyramidal neurons which receives either excitatory or inhibitory feedback from two local interneurons clusters of neurons which are composed of stellate cells, basket cells or nonpyramidal ones. These get exclusively excitatory inputs. A schematic description of the three population neural mass model representig the cortical column can be seen in Figure 1.

The correspondence with the anatomical structure of the cortical column, as it has been proposed in [David], can be approximately inferred as follows: the pyramidal population are located in the infragranular layers (Layer 5 and 6) and the interneurons clusters are tracked down to supragranular layers (Layers 1, 2 and 3) for the inhibitory cells, while the excitatory ones to granular layer (Layer 4).

It is worth mentioning that the influence from distant populations or neighboring ones is modeled as an excitatory input. Moreover, it is also well established that the EEG recordings represent measurements of the the electrical activity of the the pyramidal population.

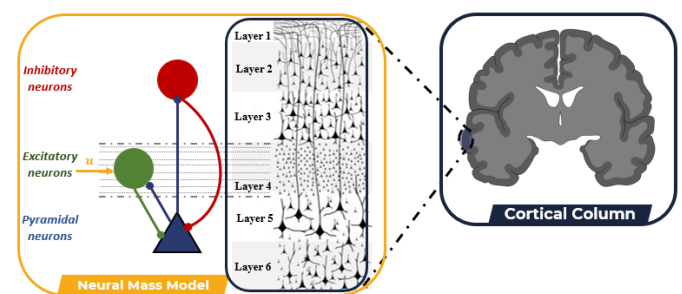


Fig. 1. Cortical column description: 3 populations neural mass model - Jansen Rit model. Figure partially created with Biorender.com.

2.2 Convolution-based Model

The dynamics of each population is described using the convolution operation as illustrated in Figure 2. In one instance, a linear transfer function traces the conversion of the pre-synaptic information into the post-synaptic one, while, in a second instance, a static nonlinear function translates the post-synaptic information into the firing

rate of the population. These conversions are based upon two operators which are detailed next:

- (1) Pulse-to-wave operator: its goal is to convert the average density of pre-synaptic input (average incoming firing rate), $m(t)$, entering the population, into the average post-synaptic potential (PSP), $v(t)$. This transformation is ensured by the linear convolution operation, as follows:

$$\begin{aligned} v(t) &= h(t) * m(t) \\ &= \int_0^{\infty} h(t-\tau)m(\tau)d\tau \end{aligned} \quad (2)$$

where $h(t)$ is called a synaptic kernel and describes the dynamic of the synapses and dendritic trees. It is modeled as a linear, time-invariant and causal weighting function given by the equation:

$$h(t) = H\kappa te^{-\kappa t} \quad (3)$$

where the two parameters that describe the convolution kernel are H , which represents the maximal amplitude of the PSP signal, and $\kappa = \frac{1}{\tau}$, which is the inverse of a time constant τ that sums the time rate constants of passive membrane and additional spatially distributed delays in the dendritic tree.

Furthermore, it is worth noticing that the synaptic contacts can be either inhibitory, or excitatory, which means that, based on the related input signal, it will lead to either inhibitory postsynaptic potential (IPSP), or excitatory postsynaptic potential (EPSP). Briefly, EPSPs will make a neuron more likely to fire, while IPSPs will make it less so. To that end, it is useful to differentiate between the inhibitory and excitatory synaptic kernels of the neuronal populations. Consequently, the former will have associated the letter (i), while the latter will include (e) as a subscript for all the related notations. Thus, the weighting functions will become $h_i(t)$, $h_e(t)$, and their parameters will be consider as H_i , τ_i , κ_i , H_e , τ_e , κ_e .

Finally, one can notice that the Laplace transform of the equation (2) leads to transfer function of a second order system describing the input-output behavior between $m(t)$ and $v(t)$, based on the kernel synaptic description given in the equation (3). Therefore, the state space representation of the synaptic connection, in a population sense, is modeled as:

$$\begin{aligned} \dot{v}(t) &= i(t) \\ \dot{i}(t) &= -\kappa^2 v(t) - 2\kappa i(t) + H\kappa m(t) \end{aligned} \quad (4)$$

where the state variables, $v(t)$ and $i(t)$, represent the mean membrane potential of the neuronal population, and its electrical current. The same distinction in notations, between excitatory and inhibitory, is applied as well.

- (2) Wave-to-pulse operator: its role is to convert the average membrane potential of the population, into the average rate of action potentials fired by the neurons. A static nonlinear sigmoid function will ensure this conversion:

$$\sigma(v(t)) = \frac{2e_0}{1 + e^{r(v_0 - v(t))}} \quad (5)$$

where the parameters e_0 , r and v_0 determine the shape of the sigmoid function, and they can be estimated using anatomically informed data based on specific intrinsic connections, the number of synapses, voltage sensitivity of the population, etc. This transformation is assumed to be instantaneous.

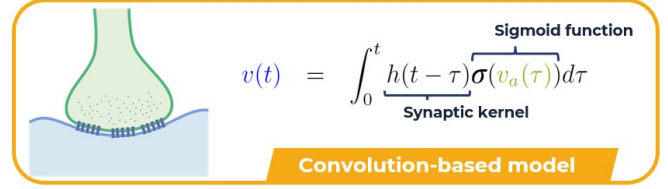


Fig. 2. Convolution-based model: it is composed by a *linear transfer function* that converse the pre-synaptic information into the post-synaptic one, and a *static nonlinear function* that translates the post-synaptic information into the firing rate of the population. Figure partially created with Biorender.com.

2.3 Neural mass model of a cortical column for epileptic seizure simulation

The neural mass model of the epileptic activity has been presented in Wendling et al. (2000) and Touboul et al. (2011). It is derived based on the Jensen-Rit model which has been introduced in Jansen and Rit (1995), and briefly described above. The mathematical representation of the cortical column that mimics an epileptic seizure using a convolution-based model is given as follows:

$$\begin{aligned} \dot{v}_1(t) &= i_1(t) \\ \dot{i}_1(t) &= \kappa_e H_e \gamma_1 \sigma(v_2(t) - v_3(t)) - \kappa_e^2 v_1(t) - 2\kappa_e i_1(t) \\ \dot{v}_2(t) &= i_2(t) \\ \dot{i}_2(t) &= \kappa_e H_e \left[\gamma_2 \sigma(\gamma_1 v_1(t)) + p(t) + u(t) \right] - \kappa_e^2 v_2(t) \\ &\quad - 2\kappa_e i_2(t) \\ \dot{v}_3(t) &= i_3(t) \\ \dot{i}_3(t) &= \kappa_i H_i \gamma_4 \sigma(\gamma_3 v_1(t)) - \kappa_i^2 v_3(t) - 2\kappa_i i_3(t) \\ y(t) &= v_2(t) - v_3(t) + n_y(t) \end{aligned} \quad (6)$$

where $x^T(t) = [v_1(t) \ i_1(t) \ v_2(t) \ i_2(t) \ v_3(t) \ i_3(t)]$ is the state vector containing the mean membrane potential, $v_i(t)$, and its electrical current, $i_i(t)$, (with the indices $i = \{1, 2, 3\}$) of the neuronal populations used to describe the neural mass model of the cortical column. The excitatory input, $p(t)$, represents the influence from distant populations or neighboring ones, while $u(t)$ will be the control input.

Besides the parameters of the excitatory and inhibitory synaptic kernels, the model includes a set of intrinsic connectivity constants, which are γ_1 and γ_2 (the average number if the synaptic contacts in the excitatory feedback loop), γ_3 and γ_4 (the average number of the synaptic contacts in the inhibitory feedback loop).

Finally, the output of the system is $y(t)$, which is the measured local field potential of the cortical column by the EEG sensor. More precisely, it is a mixture of EPSP and IPSP signals that describe the electrical activity if the

pyramidal neuronal population. In addition, the measurement noise introduced by the EEG sensor is modeled as a stochastic variable, $n_y(t)$. One can notice that the equation (6) is written in the form of the equation (1), and it is based on the Jansen-Rit neural mass model, where each EPSPs and IPSPs are given using the equations (4) and (5).

2.4 Linearized neural mass model of a cortical column for epileptic seizure

In order to develop the H_∞ controller and the Extended Kalman Filter estimator, one needs the linearized system of the nonlinear representation given in the equation (6), around an equilibrium. To that end, the matrices A , B and C that fully describe the state space representation of the linear system, can be obtained as:

$$\begin{aligned} \dot{x}(t) &= \left. \frac{\partial f}{\partial x}(x(t), u(t), \theta) \right|_{(x_e, u_e)} (x(t) - x_e) + \\ &+ \left. \frac{\partial f}{\partial u}(x(t), u(t), \theta) \right|_{(x_e, u_e)} (u(t) - u_e) \quad (7) \\ y(t) &= \left. \frac{\partial h}{\partial x}(x(t)) \right|_{x_e} (x(t) - x_e) \end{aligned}$$

where x_e and u_e are the values of the state and input at equilibrium. From the equation (7), it is clear that the linearized system parameters around the equilibrium point are:

$$\begin{aligned} A &= \left. \frac{\partial f}{\partial x}(x(t), u(t), \theta) \right|_{(x_e, u_e)} \\ B &= \left. \frac{\partial f}{\partial u}(x(t), u(t), \theta) \right|_{(x_e, u_e)} \quad (8) \\ C &= \left. \frac{\partial h}{\partial x}(x(t)) \right|_{x_e} \end{aligned}$$

It is worth noticing that the nonlinear part of the mathematical model describing the cortical column is the sigmoid function given in the equation (5). Therefore, to obtain the linearized system it is sufficient to get the first order Taylor approximation of the sigmoid function, around v_0 , (being the PSP when 50% firing rate is achieved):

$$\sigma(v) \approx \sigma(v_0) + \left. \frac{\partial \sigma(v)}{\partial v} \right|_{v=v_0} (v - v_0) \quad (9)$$

where the derivative of $\sigma(v)$ with respect to v around the equilibrium is:

$$\begin{aligned} \left. \frac{\partial \sigma(v)}{\partial v} \right|_{v=v_0} &= \left[\frac{2e_0 r}{1 + e^{r(v_0-v)}} \left(1 - \frac{1}{1 + e^{r(v_0-v)}} \right) \right] \Bigg|_{v=v_0} \\ &= \left[\frac{2e_0 r e^{r(v_0-v)}}{(1 + e^{r(v_0-v)})^2} \right] \Bigg|_{v=v_0} \\ &= \frac{e_0 r}{2} \end{aligned} \quad (10)$$

Finally, by combining the equation (10) and (9), the sigmoid function linearized around $v = v_0$ can be considered as:

$$\Delta \sigma(v(t)) = \delta \Delta v(t) \quad (11)$$

where the parameter $\delta = \frac{e_0 r}{2}$ represents a constant gain and $\Delta \sigma(v(t))$ and $\Delta v(t)$ are variations around the equilibrium point.

The linearized representation of the cortical column described by the neural mass model in the equation (6), having the hidden state, $x(t)$, external input, $u(t)$ and measured output, $y(t)$, is given by the following matrices:

$$\begin{aligned} A &= \begin{bmatrix} 0 & 1 & 0 & 0 & 0 & 0 \\ -\kappa_e^2 & -2\kappa_e & \kappa_e H_e \gamma_1 \delta & 0 & -\kappa_e H_e \gamma_1 \delta & 0 \\ 0 & 0 & 0 & 1 & 0 & 0 \\ \kappa_e H_e \gamma_2 \delta \gamma_1 & 0 & -\kappa_e^2 & -2\kappa_e & 0 & 0 \\ 0 & 0 & 0 & 0 & 0 & 1 \\ \kappa_i H_i \gamma_4 \delta \gamma_3 & 0 & 0 & 0 & -\kappa_i^2 & -2\kappa_i \end{bmatrix} \\ B &= [0 \ 0 \ 0 \ \kappa_e H_e \ 0 \ 0]^T \\ C &= [0 \ 0 \ 1 \ 0 \ -1 \ 0] \end{aligned} \quad (12)$$

3. H_∞ CONTROLLER DESIGN

The control application of suppressing the activity of a cortical column is a sensitive one that requires a careful consideration regarding the internal stability of the system as well, the performances of the control solution, and their robustness against the uncertainties. These are some of the reasons for which one might choose a H_∞ controller as a proposed solution for this control problem.

A brief description of the control problem in terms of block diagram can be depicted in Figure 3. It represents a classical feedback loop scheme, where P is the cortical column model given in the equation (6), W_e and W_u are the performance specifications of the control application, and K_∞ is the controller which is obtained using H_∞ tools. In addition, the relevant signals of the feedback loop are grouped as: external signals (reference signal, r , excitatory input, p and measurement noise, n), internal signals (tracking error, ε , control input, u , and system output, y) and controlled signals (z_1 and z_2). In particular, in this application, since one aims to suppress the activity of the cortical column, it means that the reference signal is considered null ($r = 0$).

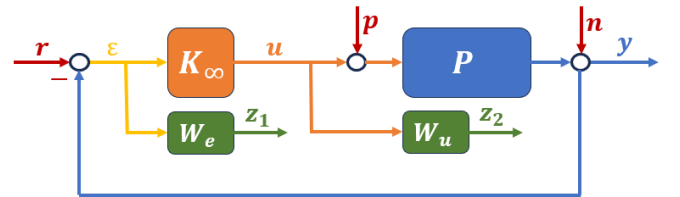


Fig. 3. Block diagram: Control problem formulation - classical feedback loop

To design the H_∞ controller, one needs the linearized model of the cortical column, which has been obtained

above. In addition, the model uncertainties are considered as additive ones and included into the equation as follows:

$$\begin{aligned} \dot{x}(t) &= Ax(t) + Bu(t) + Bp(t) + B_\sigma w_\sigma(t) \\ y(t) &= Cx(t) + n(t) \end{aligned} \quad (13)$$

where besides the system state, $x(t)$, the control input, $u(t)$, the external disturbance (excitatory input), $p(t)$, system output, $y(t)$, measurement noise, $n(t)$, and the related matrices that describe the linear system, A, B, C , there is also the additive model uncertainties given by $w_\sigma^T(t) = [w_{\sigma 1} \ w_{\sigma 2} \ w_{\sigma 3}]$, together with the associated

$$\text{matrix, } B_\sigma = \begin{bmatrix} 0 & 0 & 0 \\ H_e \kappa_e \gamma_1 & 0 & 0 \\ 0 & 0 & 0 \\ 0 & H_e \kappa_e \gamma_2 & 0 \\ 0 & 0 & 0 \\ 0 & 0 & H_i \kappa_i \gamma_4 \end{bmatrix}.$$

One can notice that the excitatory signal, $p(t)$ and the additive model uncertainties, $w_\sigma(t)$, can be grouped together as $w(t) = \begin{bmatrix} p \\ w_\sigma \end{bmatrix} (t)$, having associated the matrix

$B_1 = [B \ B_\sigma]$. This will lead to the equation:

$$\begin{aligned} \dot{x}(t) &= Ax(t) + B_1 w(t) + Bu(t) \\ y(t) &= Cx(t) + n(t) \end{aligned} \quad (14)$$

Furthermore, the performance specifications have to be considered as well. To that end, two frequency dependent templates will be proposed. On the one hand, the tracking error transfer function will be shaped by the choice of $W_e(j\omega)$, and on the other hand, the transfer function related to control input $u(t)$ is shaped by the choice of $W_u(j\omega)$ according to:

$$\begin{bmatrix} z_1 \\ z_2 \end{bmatrix} = \begin{bmatrix} W_e(j\omega) & 0 \\ 0 & W_u(j\omega) \end{bmatrix} \begin{bmatrix} \epsilon \\ u \end{bmatrix} \quad \forall \omega \in [0, \infty) \quad (15)$$

The performance specifications can be summarized by the following state space representation (with internal states $x_e(t)$ and $x_u(t)$ corresponding to transfers $W_e(s)$ and $W_u(s)$ respectively):

$$\begin{aligned} \begin{bmatrix} \dot{x}_e \\ \dot{x}_u \end{bmatrix} (t) &= \begin{bmatrix} A_e & 0 \\ 0 & A_u \end{bmatrix} \begin{bmatrix} x_e \\ x_u \end{bmatrix} (t) + \begin{bmatrix} B_e & 0 \\ 0 & B_u \end{bmatrix} \begin{bmatrix} \epsilon \\ u \end{bmatrix} (t) \\ \begin{bmatrix} z_1 \\ z_2 \end{bmatrix} (t) &= \begin{bmatrix} C_e & 0 \\ 0 & C_u \end{bmatrix} \begin{bmatrix} x_e \\ x_u \end{bmatrix} (t) + \begin{bmatrix} D_e & 0 \\ 0 & D_u \end{bmatrix} \begin{bmatrix} \epsilon \\ u \end{bmatrix} (t) \end{aligned} \quad (16)$$

In Figure 4 the lower Linear Fractional Transform (LFT) representation of the control problem illustrated in Figure 3 is given. In particular, the all templates for performance specifications are gathered in W as described in the equation (15), while the signals are grouped in the following categories: first, all the external signals, $r(t), w(t), n(t)$, in one group, second, the controlled variables, $\epsilon(t), u(t)$, that become $z_1(t), z_2(t)$ after the weights are applied, third, the control input variables, $u(t)$, and finally, the measured variable, $y(t)$.

To design the H_∞ error feedback controller, the equations (14) and (16) are combined to get:

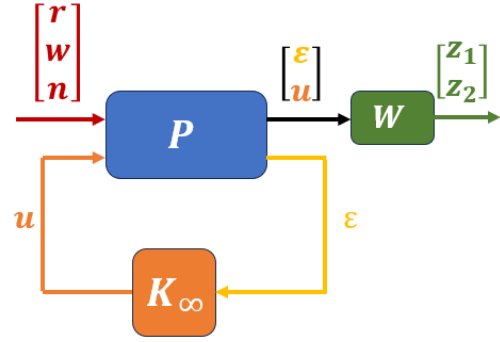


Fig. 4. Block diagram: Lower Linear Fractional Transform (LFT) of the H_∞ control problem formulation

$$\begin{aligned} \dot{\tilde{x}}(t) &= \tilde{A}\tilde{x}(t) + \tilde{B}_1\tilde{w}(t) + \tilde{B}_2u(t) \\ z(t) &= \tilde{C}_1\tilde{x}(t) + \tilde{D}_{11}\tilde{w}(t) + \tilde{D}_{12}u(t) \\ \epsilon(t) &= \tilde{C}_2\tilde{x}(t) + \tilde{D}_{21}\tilde{w}(t) \end{aligned} \quad (17)$$

where the following matrix partitions are allowed:

$$\begin{aligned} \tilde{A} &= \begin{bmatrix} A & 0 & 0 \\ -B_e C & A_e & 0 \\ 0 & 0 & A_u \end{bmatrix} & \tilde{B}_1 &= \begin{bmatrix} 0 & B_1 & 0 \\ B_e & 0 & -B_e \\ 0 & 0 & 0 \end{bmatrix} & \tilde{B}_2 &= \begin{bmatrix} B \\ 0 \\ B_u \end{bmatrix} \\ \tilde{C}_1 &= \begin{bmatrix} -D_e C & C_e & 0 \\ 0 & 0 & C_u \end{bmatrix} & \tilde{D}_{11} &= \begin{bmatrix} D_e & 0 & -D_e \\ 0 & 0 & 0 \end{bmatrix} & \tilde{D}_{12} &= \begin{bmatrix} 0 \\ D_u \end{bmatrix} \\ \tilde{C}_2 &= [-C \ 0 \ 0] & \tilde{D}_{21} &= [1 \ 0] & \tilde{D}_{22} &= 0 \end{aligned}$$

and the corresponding vectors are defined as below.

$$\tilde{x}(t) = \begin{bmatrix} x \\ x_e \\ x_u \end{bmatrix} (t) \quad \tilde{w}(t) = \begin{bmatrix} r \\ w \\ n \end{bmatrix} (t) \quad z(t) = \begin{bmatrix} z_1 \\ z_2 \end{bmatrix} (t) \quad (18)$$

Finally, a stabilizing controller is computed, if possible:

$$u(t) = K_\infty(x_K(t), \epsilon(t), t) \quad (19)$$

which is a solution of the optimization problem

$$\min_{u(t)} \left\| \begin{bmatrix} W_e S & W_e P S \\ W_u K S & W_u T \end{bmatrix} \right\|_\infty < \gamma \quad (20)$$

where $\gamma > 0$ is a given attenuation level, while S, KS, PS and T are the main classical sensitivity transfer functions. It is worth noticing that the choice of the templates $W_e(j\omega)$ and $W_u(j\omega)$ (in \mathbb{RH}_∞) actually shapes these sensitivity transfer functions.

By using a Riccati based approach (one can check Doyle et al. (2016) for more details), a solution to the problem formulated in the equation (20) in the form of the equation (19) can be computed. This solution ensures the internal stability of the system as well as the performance specification and the robustness against the model uncertainties and measurement noise.

4. STATE OBSERVER DESIGN

The goal of this section is to estimate the hidden state of a cortical column modeled as a neural mass model

for an epileptic seizure, which is described by the vector $x^T(t) = [v_1(t), i_1(t), v_2(t), i_2(t), v_3(t), i_3(t)]$, based on the available mathematical model derived earlier and the noisy measurement of an EEG sensor, $y(t)$. To that end, an Extended Kalman Filter (EKF) is designed.

The EKF observer is an auxiliary system of the form:

$$\begin{aligned} \dot{\hat{x}}(t) &= f(\hat{x}(t), u(t)) + K(y(t) - \hat{y}(t)) \\ \hat{y}(t) &= C\hat{x} \end{aligned} \quad (21)$$

where $\hat{x}(t)$ and $\hat{y}(t)$ represent the estimated state and output, respectively. The dynamics of this auxiliary system is given by the nonlinear model, $f(\bullet)$, which is chosen following the equation . It is also worth noticing that the known input, $u(t)$, will be considered as zero in this context. Moreover, the excitation signal, $p(t)$, will be modeled as the process disturbance, which can be clearly seen that it is an additive one. The estimated output, $\hat{y}(t)$, is a linear combination of the estimator's state components.

The observer is driven by a correction term which is based on the error between the measured and estimated outputs, $y(t) - \hat{y}(t)$, while the matrix K is the observer gain.

The estimation problem described hereby comes down to find K such that auxiliary system given in the equation (21) is stable and its state, $\hat{x}(t)$ converges to the system state, $x(t)$. To that end, in the EKF estimator, one can compute the observer gain, K , as the classical Kalman filter problem, namely:

$$K(t) = P(t)C^T R^{-1} \quad (22)$$

where $P(t)$ is a solution of the continuous-time Riccati differential equation:

$$P(t) = AP(t) + P(t)A^T - P(t)C^T R^{-1} CP(t) + Q \quad (23)$$

with A and C being the matrices of the linearized system obtained in the equation (12), while Q and R are the state noise and measured output noise covariance matrices, correspondent to the excitatory signal, $p(t)$, and measurement noise, $n(t)$. This equation allows to leverage the available information about the model accuracy and measurement noise. However, for the proposed solution one can use the static solution of the equation (23), which leads to a simpler implementation of the EKF observer, the so-called continuous-time algebraic Riccati equation (CARE) (one can find more details in Besancon (2007)):

$$0 = AP + PA^T - PC^T R^{-1} CP + Q \quad (24)$$

5. SIMULATION RESULTS

In the following section, the simulation results for both, the H_∞ robust controller and the EKF observer applied to the neural mass model of an epileptic seizure are provided.

The simulation scenario under which the both methods are tested starts from nonlinear description of the neural mass model of the cortical column given in the equation (6).

The standard numerical values of the parameters underling the model proposed in Wendling et al. (2000) (which are adapted from Jansen et al. (1993) and Jansen and Rit (1995)) are summarized in Table 1. It is worth mentioning that, if one is interested to simulate an epileptic behaviour of a cortical column, then a group of hyper-excitatory parameters ought to be chosen such for the neural mass model. In particular, for the current simulation scenario the value of the average synaptic excitatory gain, H_e , has been set to 7.00 mV.

Table 1. Parameters description and numerical values of the neural mass model of a cortical column (nominal case) adapted from Wendling et al. (2000)

Param.	Value	Interpretation
H_e	3.25 mV	Average synaptic gain (excitatory)
H_i	22.00 mV	Average synaptic gain (inhibitory)
τ_e	0.01 s	Membrane average time constant and dendritic tree average time delays (excitatory)
τ_i	0.02 s	Membrane average time constant and dendritic tree average time delays (inhibitory)
γ_1	135	Average number of synaptic contacts in the excitatory feedback loop
γ_2	108	Average number of synaptic contacts in the excitatory feedback loop
γ_3	33.75	Average number of synaptic contacts in the inhibitory feedback loop
γ_4	33.75	Average number of synaptic contacts in the inhibitory feedback loop
e_0	2.5 s ⁻¹	Nonlinear sigmoid function parameter
v_0	6 mV	Nonlinear sigmoid function parameter
r	0.56 mV ⁻¹	Nonlinear sigmoid function parameter

5.1 H_∞ robust controller simulation results

Based on the H_∞ controller design presented in section 3, the results obtained are illustrated hereby, as follows:

First, one can notice that the performance specifications of the control problem have to be set. More specifically, the templates $W_e(j\omega)$ and $W_u(j\omega)$ from the equation (15) are chosen as illustrated in Figure 5 and 6. In particular, W_e has the shape of a low pass filter, for which its parameters are specified such that the error signal, $\varepsilon(t)$, has to rest under the value of 0.1 in magnitude (20 dB) given the frequency range of [0, 44] rad/sec. In addition, the maximum value of the closed loop sensitivity function has to be less than 6dB to ensure an acceptable robustness regarding the stability margin of the closed loop system, taking into account that model uncertainties have been modeled as additive ones.

Next, the template $W_u(j\omega)$ has been shaped as a high pass filter. In this case, its role is, mainly, to ensure that the control input will not be larger than a certain value, so as not to damage the neural tissue.

Its shape can be modified, if necessary, depending on additional requirements concerning the control input constraints or other closed loop transfers related to this template.

Next, one can notice that the linearized system obtained in the equation (7), having the corresponded matrices

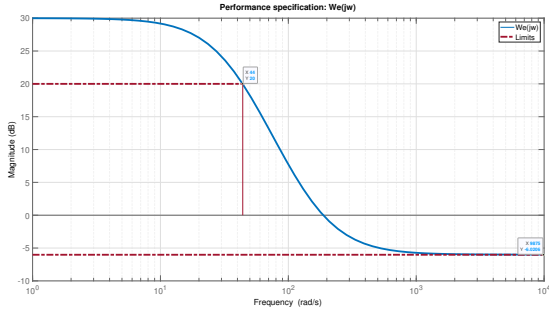


Fig. 5. H_∞ controller design: Performance specification for the tracking error signal - $W_e(j\omega)$

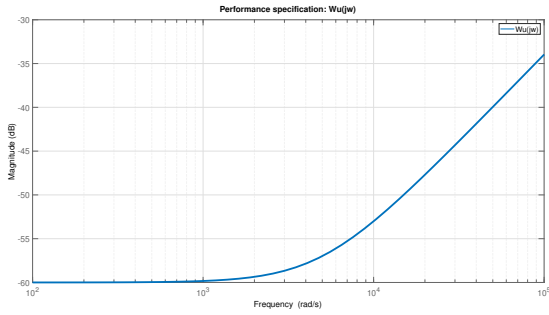


Fig. 6. H_∞ controller design: Performance specification for the control input signal - $W_u(j\omega)$

given by the equation (12), under the parameters described above is both controllable and observable.

Furthermore, by solving the optimization problem given in the equation (17), one will get an H_∞ controller as in the equation (19) for an attenuation level, $\gamma = 0.9953$. This imply that the obtained controller will indeed ensure the stability of the system for which it was designed as well as the performance specifications described by the chosen templates. This, of course, can also be seen in Figure 7, 8, 9 and 10 where all the closed loop sensitivity functions, namely, $S(j\omega)$, $PS(j\omega)$, $KS(j\omega)$ and $T(j\omega)$ are bounded by the $W_e(j\omega)$ respectively the $W_u(j\omega)$.

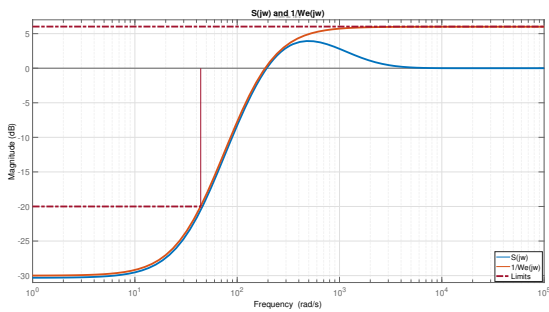


Fig. 7. H_∞ controller results: Performance specification template $W_e(j\omega)^{-1}$ (orange) and closed-loop sensitivity function $S(j\omega)$ (blue)

Finally, the obtained H_∞ controller is tested using the nonlinear model of the cortical column. The results of the simulation are shown Figure 11. It can be seen that for the first 5 sec the controller is deactivated, and after that it

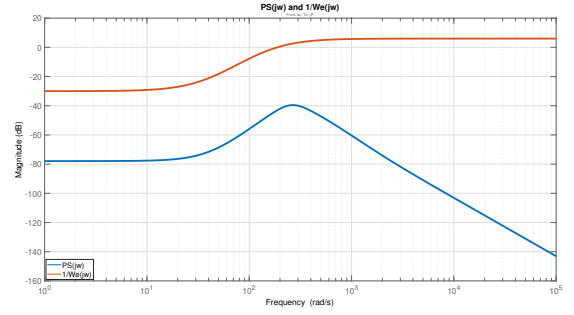


Fig. 8. H_∞ controller results: Performance specification template $W_e(j\omega)^{-1}$ (orange) and closed-loop disturbance sensitivity function $PS(j\omega)$ (blue)

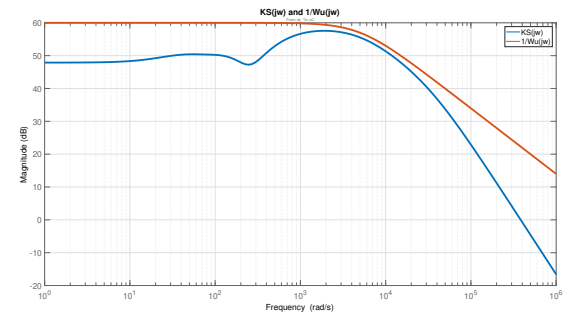


Fig. 9. H_∞ controller results: Performance specification template $W_u(j\omega)^{-1}$ (orange) and closed-loop control sensitivity function $KS(j\omega)$ (blue)

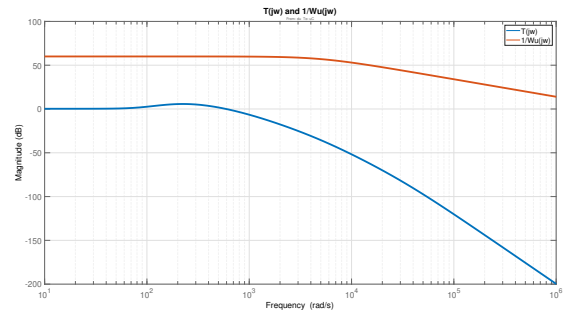


Fig. 10. H_∞ controller results: Performance specification template $W_u(j\omega)^{-1}$ (orange) and closed-loop complementary function $T(j\omega)$ (blue)

is switched on. Once that happens, the epileptic activity is suppressed. One can notice that in the first simulation the measured output is noise free. Thus, if a measurement noise is added, the controller still behaves well enough, managing to achieve its goal, in other words to suppress the epileptic seizure, as it can be seen in Figure 12.

5.2 Extended Kalman Filter simulation results

In this section, the results of the estimation problem are shown. In particular, the state estimates of the EKF observer are compared against the real ones simulated by the nonlinear model of the cortical column described by the equation (6).

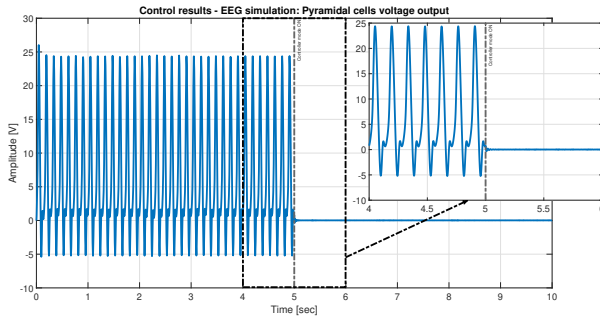


Fig. 11. H_∞ controller results: EEG simulated recordings without measurement noise included. Controller switched ON after $t = 5$ sec. A zoomed graphic of the results in the interval $[4, 6]$ sec is displayed in top-right side of the figure

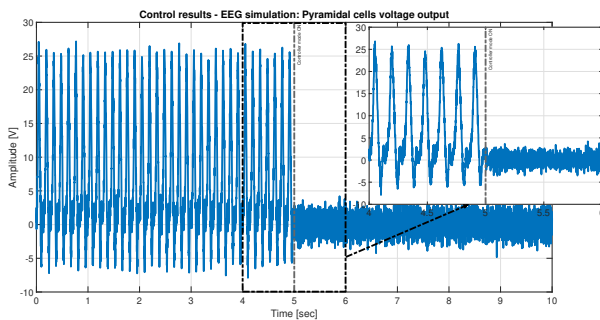


Fig. 12. H_∞ controller results: EEG simulated recordings with measurement noise included. Controller switched ON after $t = 5$ sec. A zoomed graphic of the results in the interval $[4, 6]$ sec is displayed in top-right side of the figure

One can notice again that the observability condition is fulfilled, therefore design of the EKF can be pursued. As it is mentioned in the equation (21), the auxiliary system that plays the role of the estimator, incorporates the nonlinear model of the cortical column described by the equation (6) and adds a correction term which depends by the observer gain and the error between the noisy output of the system and the estimated one. The gain, in this scenario, is considered as being constant and it is computed solving the continuous-time algebraic Riccati equation as given in (24). This equation is composed of the matrices obtained by linearizing the nonlinear system of the cortical column, and the state and noise covariance matrices, Q and R . These matrices are chosen based on the state disturbances and measurement noise signals. Since $y(t)$ and $p(t)$ are one dimensional external inputs, it means that the covariance matrices will be scalars. In particular, based on the parameters of the simulation, $Q = 5 \cdot 10^6$ and $R = 10$. By choosing these matrices, one can ensure a trade off between the system output and the available model.

Based on EKF solution of the estimation problem combining the nonlinear model of the cortical column with the noisy recordings of an EEG sensor placed on top of the cortical column, and using the numerical values described in this section, the state estimates of the unmeasured activity of the cortical column can be obtained. In

particular, in Figure 13 the EEG recording, $y(t)$ together with its estimate, $\hat{y}(t)$ are shown. In Figure 14, the mean membrane voltage potential (in population sense), $v_1(t)$ and its estimate, $\hat{v}_1(t)$, are illustrated, while in Figure 15, the other membrane voltage of the excitatory neuronal population, $v_2(t)$ and its estimate, $\hat{v}_2(t)$ are given. Finally, the voltage potential of the inhibitory population, $v_3(t)$ and its estimate, $\hat{v}_3(t)$ is depicted.

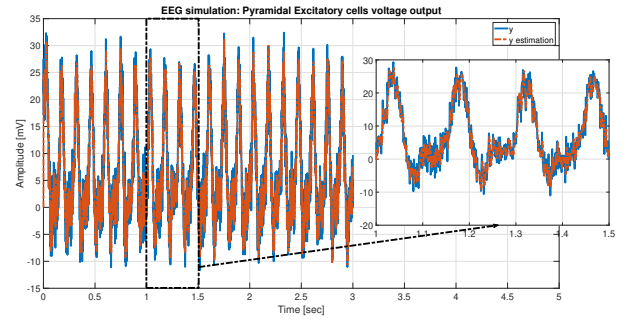


Fig. 13. EKF observer results: EEG simulated recordings, $y(t)$, system output (blue) and observer estimated output, $\hat{y}(t)$ (orange)

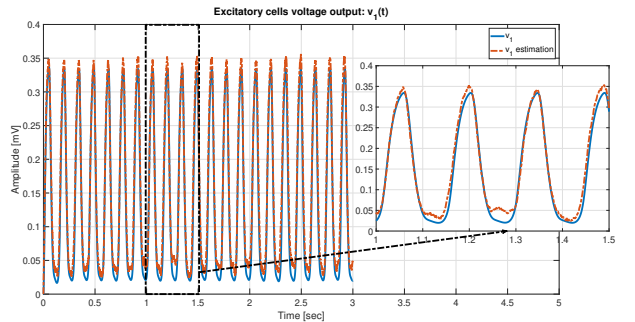


Fig. 14. EKF observer results: cortical column simulated state, $v_1(t)$, hidden state (blue) and observer estimated state, $\hat{v}_1(t)$ (orange)

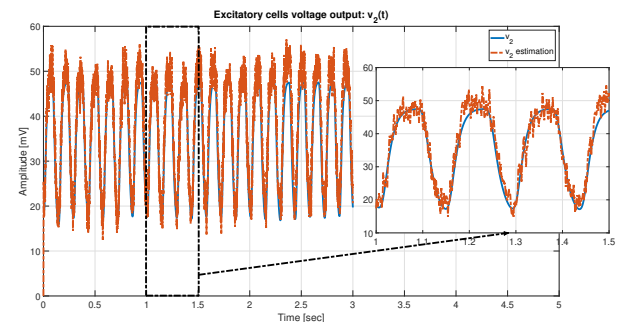


Fig. 15. EKF observer results: cortical column simulated state, $v_2(t)$, hidden state (blue) and observer estimated state, $\hat{v}_2(t)$ (orange)

6. CONCLUSIONS

The paper presented the design of a H_∞ controller and an Extended Kalman Filter observer applied to a neural mass model for EEG recordings of a cortical column. Both methods were tested, in simulation, on a model of

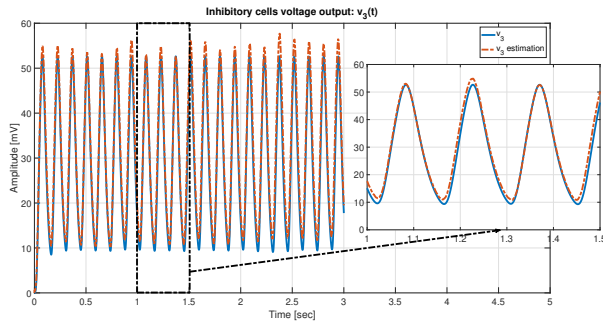


Fig. 16. EKF observer results: cortical column simulated state, $v_3(t)$, hidden state (blue) and observer estimated state, $\hat{v}_3(t)$ (orange)

an epileptic seizure. The objective of the controller has been to suppress the activity of the cortical column, while the observer has been deployed to estimate the hidden, unmeasured activity of the cortical column. Both methods have been designed based on the linearized model of the neural mass model and deployed for the nonlinear one. The model uncertainties have been considered as additive ones during the design process. The measurement noise introduced by the EEG sensors has been accounted as well. The results obtained in simulation are promising and motivate the authors to extend this work for real time EEG recordings.

Finally, as further work, these methods will be considered for larger networks of cortical columns. Moreover, regarding the model and parameters uncertainties the design process will be refined. In particular, for the former other manners to model the uncertainties will be tested, while for the latter, the H_∞ control problem solution will take them into account as well.

In addition, one might choose a fractional order model to describe the EEG recordings due to its fractal nature. Therefore, it will be useful to investigate how these type of models can be integrated with the H_∞ control solution presented hereby.

ACKNOWLEDGEMENTS

The results presented in this paper, on the one hand, have been funded by the Ministry of Investments and European Projects through the Human Capital Sectoral Operational Program 2014-2020, Contract no. 62461/03.06.2022, SMIS code 153735, and on the other hand, supported by a grant of the Ministry of Research, Innovation and Digitization, CNCS-UEFISCDI, project number PN-III-P1-1.1-PD-2021-0285, within PNCDI III.

REFERENCES

Besancon, G. (2007). *An Overview on Observer Tools for Nonlinear Systems*. Springer Berlin, Heidelberg.
 David, O. and Friston, K.J. (2003). A neural mass model for meg/eeeg coupling and neuronal dynamics. *NeuroImage*, 20, 1743–1755.
 David, O., Kiebel, S.J., Harrison, L.M., Mattout, J., Kilner, J.M., and Friston, K.J. (2006). Dynamic causal modeling of evoked responses in eeg and meg. *NeuroImage*, 30, 1255–1272.

Deschle, N., Gossn, J.I., Tewarie, P., Schelter, B., and Daffertshofer, A. (2021). On the validity of neural mass models. *Frontiers in Computational Neuroscience*, 14.
 Doyle, J., Glover, K., Khargonekar, P., and Francis, B. (2016). State-space solutions to standard h_2 and h_∞ control problems. *IEEE Transaction on Automatic Control*, 34, 831–847.
 Glomb, K., Cabral, J., Cattani, A., Mazzoni, A., Raj, A., and Franceschiello, B. (2022). Computational models in electroencephalography. *Brain Topography*, 35, 142–161.
 Hamid, M.H.A., Postoyan, R., and Daafouz, J. (2015). Local observers design for a class of neural mass models. *European Control Conference, Linz, Austria*.
 Hodgkin, A.L. and Huxley, A.F. (1952). A quantitative description of membrane current and its application to conduction and excitation in nerve. *The journal of Physiology*, 117, 500–544.
 Jansen, B.H. and Rit, V.G. (1995). Electroencephalogram and visual evoked potential generation in a mathematical model of coupled cortical columns. *Biological Cybernetics*, 74, 357–366.
 Jansen, B.H., Zouridakis, G., and Brandt, M.E. (1993). A neurophysiologically-based mathematical model of flash visual evoked potentials. *Biological Cybernetics*, 74, 357–366.
 Kuhlmann, L., Freestone, D.R., Manton, J.H., Heyse, B., Vereecke, H.E.M., Lipping, T., Struys, M.M.R.F., and Liley, D.T.J. (2016). Neural mass model-based tracking of anesthetic brain states. *NeuroImage*, 133, 438–456.
 Moran, R., Pinotsis, D.A., and Friston, K. (2013). Neural masses and fields in dynamic causal modeling. *Frontiers in Computational Neuroscience*, 7, 1–12.
 Moran, R.J., Kiebel, S.J., Stephan, K.E., Reilly, R.B., Daunizeau, J., and Friston, K.J. (2007). A neural mass model of spectral responses in electrophysiology. *NeuroImage*, 37, 706–720.
 Pereira, I., Frässle, S., Heinzle, J., Schöbi, D., Do, C.T., Gruber, M., and Stephan, K.E. (2021). "conductance-based dynamic causal modeling: A mathematical review of its application to cross-power spectral densities. *NeuroImage*, 245.

Popescu, A. and Buiu, C. (2023). Mean membrane potential estimation for neural mass models in eeg recordings using a linear state observer. *11th International Conference on E-Health and Bioengineering, Bucharest, Romania*.
 Touboul, J., Wendling, F., Chauvel, P., and Faugeras, O. (2011). Neural mass activity, bifurcations, and epilepsy. *Neural Computation*, 23, 3232–3286.
 Wang, J., Niebur, E., Hu, J., and Li, X. (2016). Suppressing epileptic activity in a neural mass model using a closed-loop proportional-integral controller. *Scientific reports* 6, 27344.
 Wei, W., Wei, X., Zuo, M., Yu, T., and Li, Y. (2019). Seizure control in a neural mass model by an active disturbance rejection approach. *International Journal of Advanced Robotic Systems*, 16, 1–15.
 Wendling, F., Bellanger, J.J., Bartolomei, F., and Chauvel, P. (2000). Relevance of nonlinear lumped-parameter models in the analysis of depth-eeg epileptic signals. *Biological Cybernetics*, 83, 367–378.